A STUDY OF SOME APPROACHES TO VIBRATION DATA ANALYSIS

T. ABRAHAMSSON*, T. MCKELVEY and L. LJUNG****

*Saab Military Aircraft, S-581 88 Linköping, Sweden
**Department of Electrical Engineering, Linköping University, S-581 83 Linköping, Sweden

Abstract. Using data from extensive vibrational tests of the new aircraft Saab 2000 three different methods for vibration analysis are studied. These methods are ERA (eigensystem realization algorithm), N4SID (a subspace method) and PEM (prediction error approach). We find that both the ERA and N4SID methods give good initial model parameter estimates that can be further improved by the use of PEM. We also find that all methods give good insights into the vibrational modes.

Key Words. System identification, modal analysis, state-space methods, application.

1. INTRODUCTION

Analysis of vibrating structures is a very important industrial task. This concerns both tests and analysis for validating safety and comfort properties and most often involves analyzing structural modes and damping properties.

A large number of methods for this have been developed and the area is both commercially important and scientifically interesting. The area has, however, historically not been closely related to the traditional System Identification methodology.

In this contribution we will study some methods for vibration analysis and evaluate the results obtained. The data we worked with is from rather extensive tests with the new commercial aircraft Saab 2000, developed by the Saab Aircraft company.

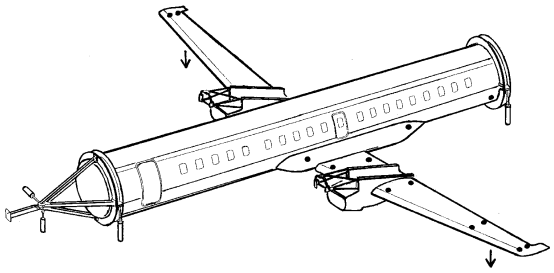

Fig. 1. Test specimen. Location of wing and fuselage accelerometers are shown as dots (nacelle accelerometers are not shown). All shown accelerometers sensing vertical accelerations. Arrows indicate location of snap-back cables.

2. THE EXPERIMENT

The experimental results presented herein are part of a large-scale experimental damping survey performed on the Saab 2000. The study was aimed at revealing the damping properties and their dependence on deformation of a body-in-green fuselage/wing/nacelle assembly (see Figure 1). It was suspected before the test, and verified and quantified by the test, that the damping would increase with increasing vibrational magnitude. The test was divided into two phases, the first consisting of a conventional ground vibration (normal mode) test at a low vibrational level and under stationary harmonic condition. The second phase was a complementary high vibrational level study. The results of the test were to be applied in the aircraft load evaluation and simulation of extremely hard landings (up to 3 m/s sink rate). The results presented in this paper are mainly from the second phase of the test.

Various excitation locations and magnitudes were used during the second phase. Snap-back excitations from pre-determined deflection states were used as structural inputs. Accelerometers and load cells were used to sense the structural response. An enormous amount of data were collected during the test, out of which a selected amount has been used in this paper. The results presented here were obtained during a wing-tip snap-back excitation from a moderate initial deflection state (10% of the highest excitation level used). In this test 21 accelerometers were distributed over the wings (12 accelerometers), the nacelles (6) and fuselage (3). Load cells were used to register the reactive loads on the supports and tension in the pre-stressed cables used for excitation. A sampling rate of 512 Hz was used.

In the first phase of the test, a resonance search and normal mode test was performed. The resonance frequencies (in the frequency range from 0 to 40 Hz), modal dampings and normal modes of the test specimen were obtained at a low vibrational level. Results from the two test phases are compared in the results section of this paper.

3. IDENTIFICATION METHODS

Consider the linear time-invariant discrete time state-space model

$$\begin{aligned} x(t+1) &= Ax(t) + Bu(t) \\ y(t) &= Cx(t) + Du(t) \end{aligned}, \qquad (1)$$

where $y(t) \in \mathbb{R}^p$, $u(t) \in \mathbb{R}^m$ and $x(t) \in \mathbb{R}^n$ with n equal the order of the system. In (1) we let the time t be normalized with the sampling period. Assuming all modes are sub-critically damped, the number of mode pairs described by this model is thus $n/2$ where each mode is associated with a complex conjugate eigenvalue pair of the matrix A.

Given, probably noisy, measured data $y_t, u_t,\ t = 0, \ldots, N-1$ from an experiment performed on the system, the aim of the identification process is to yield estimates of A, B, C and D in (1) such that the fit to measured data

$$V = \frac{1}{N} \sum_{t=0}^{N-1} |y_t - y(t)|^2 \tag{2}$$

is good.

In this paper we will briefly describe three different approaches to solve the stated problem above and discuss some fine tuning which can be applied to further improve the result.

3.1. *ERA*

The eigensystem realization algorithm (ERA), introduced by Juang and Pappa (1985), can be used if the measured data is from the free decaying motion following upon an initial excitation. The algorithm is based on the early realization result by Ho and Kalman (1966), and utilizes the rank deficiency property of the block Hankel matrix constructed by the impulse response of the system. For real measured data the Hankel matrix is generally always of full rank and a singular value decomposition (SVD) is used to infer an appropriate lower rank approximation.

Assume we are given $N = q + r$ measurements y_t resulting from a free decaying motion started at time $t = 0$. Construct the 2 block-Hankel matrices

$$Y_{qr}(t) = \begin{bmatrix} y_t & y_{t+1} & \cdots & y_{t+r-1} \\ y_{t+1} & \vdots & \cdots & \vdots \\ \vdots & \vdots & \vdots & \vdots \\ y_{t+q-1} & y_{t+q} & \cdots & y_{t+q+r-2} \end{bmatrix} \tag{3}$$

$t = 1, 2$, where $q > n$ and $r \geq n$ is the number of block rows and columns respectively. Form the singular value decomposition

$$Y_{qr}(1) = \begin{bmatrix} \hat{U}_1 & \hat{U}_2 \end{bmatrix} \begin{bmatrix} \hat{\Sigma}_1 & 0 \\ 0 & \hat{\Sigma}_2 \end{bmatrix} \begin{bmatrix} \hat{V}_1^T \\ \hat{V}_2^T \end{bmatrix} \tag{4}$$

where the diagonal matrix $\hat{\Sigma}_1$ contains the n principal singular values. If we assume that y_t is noise-free and originates from (1), $Y_{qr}(1)$ will be of rank n and hence $\hat{\Sigma}_2 = 0$. A realization of (1) is then calculated as

$$E_p^T = [\, I_p \ 0_p \ \ldots \ 0_p \,],\ E_m^T = [\, I_m \ 0_p \ \ldots \ 0_p \,] \tag{5}$$

$$\hat{A} = \hat{\Sigma}_1^{-1/2} \hat{U}_1^T Y_{q,r}(2) \hat{V}_1 \hat{\Sigma}_1^{-1/2} \tag{6}$$

$$\hat{B} = \hat{\Sigma}_1^{1/2} \hat{V}_1^T E_m,\ \hat{C} = E_p^T \hat{U}_1 \hat{\Sigma}_1^{1/2},\ \hat{D} = y_0 \tag{7}$$

where I_i denotes the $i \times i$ identity matrix and 0_i denotes the $i \times i$ zero matrix. The estimated system $(\hat{A}, \hat{B}, \hat{C}, \hat{D})$ are then related to the original system (A, B, C, D) by a similarity transformation. If we use this algorithm on noisy data or data from a high order system $\hat{\Sigma}_2$ will not be identically zero and $(\hat{A}, \hat{B}, \hat{C}, \hat{D})$ will then be an approximation of the true system. This approximation does not necessarily minimize (2). However, in general ERA has been experienced to provide models which are close to the minimum.

3.2. *N4SID - a subspace method*

This method is recently developed by Van Overschee and De Moor, see Van Overschee and De Moor (1994). The method handles arbitrary inputs $u(t)$ and also estimates a noise model and is thus much more general than ERA. The algorithm determines a state sequence through an approximate projection of input and output data. From the state sequence obtained, it is easy to calculate a minimal state-space model of the system (1) including a stochastic rational model of the noise.

We used the N4SID (algorithm 2) and changed the default division between past and future data such that the past was changed to be as long as the duration of the exciting input signal. This change was made to better allow for short duration input.

3.3. *Prediction Error Methods*

The prediction error methods (PEM) contain the most known and used methods for system identification and has been developed and analyzed extensively during the last three decades. For a unifying treatment we refer to Ljung (1987).

Here we will concentrate on the state-space model (1). Since a noise model is not included, the model (1) is commonly referred to as an output-error form.

The state-space system matrices (A,B,C,D) are parameterized using a parameter vector θ to obtain the predictor $\hat{y}(t|\theta)$. A minimal number of parameters needed is given by the multivariable identifiable forms, also called canonical forms, see Ljung (1987).

The parameter vector and hence the model is then obtained by minimizing the squared sum of the prediction errors

$$\hat{\theta} = \arg\min_{\theta} \frac{1}{N} \sum_{t=1}^{N} |y_t - \hat{y}(t|\theta)|^2 \tag{8}$$

This minimization is in general nonlinear in the parameters θ and has to solved by an iterative method, *e.g.* a Gauss-Newton algorithm. The success of this approach is to a large extent dependent on the initial estimate from which the iterative method is started. This fact becomes increasingly significant as model complexity grows.

3.4. *Improvements of the estimate*

The two first methods ERA and N4SID is fundamentally different from PEM since they lack an explicit criterion of the type (2). For a finite number of measurements and noisy data we cannot guarantee that ERA or N4SID are optimal in any sense. However based on the results from applying these methods on real data we believe that ERA and N4SID give quite good initial estimates which often can be improved by minimizing a prediction error criterion (8). Experience shows that B and D estimates often are of lower quality compared with the estimates of A and C for N4SID if the input has a low degree of excitation. However B and D can easily be re-estimated by minimizing (2). Notice that B and D then are linear in $y(t)$ and, for fixed A and C, simply can be estimated by an ordinary least-squares

solution.

If further improvements are needed we can estimate all the system matrices by (8) with *e.g.* Gauss-Newton iterations using the previously estimated model as an initial estimate, preferably converted with a similarity transformation to some proper form suited for a small parameterization. This last step would thus provide a model with best variance properties if certain assumptions are made on the noise, see Ljung (1987). The degree of improvement is application dependent and has, using data from various experiments, been observed to vary from a 50% reduction of (2) to only marginally improvements.

3.5. *Near minimal parameterization*

Physical insight into the problem here at hand gives that, for the low-damped structure under test, overdamped modes should be neglected. Any such mode found during the identification process is most likely a "computational" mode representing noise in the data. Thus only complex conjugate subcritically damped modes are retained in the model. If we assume A to be non-deficient this implies that the n real states given by ERA and N4SID algorithms can be transformed into n decoupled complex conjugate states out of which only $n/2$ are required for a full analysis. The real system equations are thus transformed into complex ones where the matrices are given by the complex similarity transform T, which converts A to a diagonal matrix $\tilde{A}$ with the complex eigenvalues on the diagonal, $\tilde{A} = T^{-1}AT$, $\tilde{B} = T^{-1}B$ and $\tilde{C} = CT$. One should notice that half the states are the complex conjugate of the other half and hence are redundant. Using complex arithmetic only $n/2$ states thus need to be considered. Furthermore, since all states are fully decoupled the computational load when solving the system equations (1) is minimized. This is extremely useful when using PEM or in a possible least-squares calculation of $\tilde{B}$ and D.

The load/acceleration relation of a mechanical system implies certain relations on the system matrices. Defining $P = \tilde{C}\tilde{A}^{-1}$ one has for measured accelerations

$$\tilde{C} = P\tilde{A}, \quad D = P\tilde{B}. \tag{9}$$

One can notice that the total number of real valued parameters required to characterize the complex valued system matrices thus is $n(m + p + 1)$. These are the n parameters of $\tilde{A}$, (recall all eigenvalues appear in complex conjugate pairs), the nm parameters of $\tilde{B}$ and the np parameters of P. A theoretical minimal parameterization is obtained by a canonical form which requires $n(m + p)$ number of parameters, see Ljung (1987). A canonical parameterization however does not possess the decoupled property as the one described. Physical insights are also lost since the parameters only implicitly define the eigenvalues and mode shapes.

3.6. *System order selection*

An important user choice is the number of states, or modes, to use in (1). The presence of noise and structural nonlinearities usually make the Hankel matrix (3) of full rank. However, if a clear gap exists among the largest and the smallest singular values of (4), it is natural to regard the largest singular values as originating from the linear system and the smallest ones from noise and nonlinearities. This approach is applicable using ERA or N4SID in which a similar SVD is performed.

An approach more closely related to the modes is by use of the measure Modal Amplitude Coherence, γ, introduced in Juang and Pappa (1985). Recall (7). The estimated B matrix can thus be expressed as

$$T^{-1}\hat{\Sigma}_1^{1/2}\hat{V}_1^T E_m = \tilde{B} \tag{10}$$

using the similarity transformation T which diagonalize A. Construct the complex controllability matrix

$$\mathcal{C} = [\tilde{B}, \tilde{A}\tilde{B}, \ldots, \tilde{A}^{r-1}\tilde{B}] \tag{11}$$

which also can be seen as the time sequence of the complex states resulting from an impulse input. Notice that row j in $\mathcal{C}$ corresponds to eigenvalue j. Define the matrix

$$\bar{\mathcal{C}} = T^{-1}\hat{\Sigma}_1^{1/2}\hat{V}_1^T \tag{12}$$

which is the controllability matrix induced by the measured data and the SVD (4). The coherence parameter γ_j corresponding to eigenvalue j is defined as

$$\gamma_j = \frac{|\bar{\mathcal{C}}_j \mathcal{C}_j^*|}{(|\bar{\mathcal{C}}_j \bar{\mathcal{C}}_j^*||\mathcal{C}_j \mathcal{C}_j^*|)^{1/2}} \tag{13}$$

where the subscript denotes row number and $(\cdot)^*$ denotes conjugate transpose. The parameter γ_j takes values between 0 and 1. Large values thus denote a high degree of coherence.

The Modal Amplitude Coherence indicator can be used in a stabilizing diagram to visualize frequency location and modal accuracy for each model order estimated. In a stabilizing diagram a bar of length γ_j is plotted for each mode and at the level corresponding to the model order (see figure 4). The characteristics of the diagram is that for identified models with too few states some identified frequencies have low indicators (the bars are short). As the model order increases these split into two or more modes with higher coherence indicators. As the model order increases the identified frequencies "stabilize", hence the name stabilizing diagram.

The modal Amplitude Coherence is defined only for ERA. For N4SID we can obtain an approximation which will be of high quality if the number of outputs are close to the number of states and if $\tilde{C}$ has full rank. In this case we define

$$\tilde{\mathcal{C}} = \tilde{C}^{\dagger}[y_1, y_2, \ldots, y_r] \tag{14}$$

where $(\cdot)^{\dagger}$ denotes the Moore-Penrose pseudo-inverse. An approximate Modal Amplitude Coherence, $\tilde{\gamma}_j$ is then derived as

$$\tilde{\gamma}_j = \frac{|\tilde{\mathcal{C}}_j \mathcal{C}_j^*|}{(|\tilde{\mathcal{C}}_j \tilde{\mathcal{C}}_j^*||\mathcal{C}_j \mathcal{C}_j^*|)^{1/2}} \tag{15}$$

3.7. *Validation*

An important part of the identification process is to assess the quality of the estimated model. If several experiments are performed on the same system under similar conditions we can use one set of measurements for estimation and use the other independent set to validate the model. If only one data set is available but consists of a large number of outputs (here accelerometer measurements) we can divide the outputs into two disjoint sets. If the division is made such that all modes are present in both sets

we can estimate a model using only one set of outputs and validate using the other set. In this paper we have used this latter method.

Assume the estimated model is given by $(\hat{A},\hat{B},\hat{C},\hat{D})$ derived using the estimation output set. To validate this model, we estimate $\hat{C}_v$ and $\hat{D}_v$ using the validation outputs. Since both matrices are linear in the outputs, given $\hat{A}$ and $\hat{B}$, $\hat{C}_v$ and $\hat{D}_v$ are calculated by minimizing (2) using an ordinary least-squares solution.

As a measure of model quality we will use

$$Q = 1 - \sqrt{\frac{\sum_{t=0}^{N-1} |y_t - \hat{y}(t)|^2}{\sum_{t=1}^{N} |y_t|^2}} \tag{16}$$

which is a normalized estimation error where increasing values of Q indicate better fit and 1 indicates a perfect fit of the model to the validation data.

The conventional ground vibrational test (GVT) also gives estimates of frequencies and modal shapes at each measurement point. These estimates can be used to validate the linear models obtained by ERA, N4SID and PEM. The modal assurance criterion (MAC) can be evaluated for each identified frequency against the results obtained in the GVT. MAC is defined as the correlation between the modal vectors of the two different models evaluated for each frequency

$$\mathrm{MAC}_k = \frac{(\tilde{c}_k^* g_k)^2}{(\tilde{c}_k^* \tilde{c}_k)(g_k^* g_k)} \tag{17}$$

where $\tilde{c}_k$ is the kth column of $\tilde{C}$ and g_k is the corresponding modal vector obtained in the GVT. An analogue definition is used for the correlation betweeen modes of ERA and N4SID.

3.8. *Frequencies and Dampings*

The estimated model is now an abstract model of the experimental data. Particularly, the eigenvalues of the matrix $\hat{A}$ give us information about frequency and damping ratio for all identified structural modes. Denote sampling frequency with f given in Herz and $\lambda_k(\tilde{A})$, $k = 1, \ldots, n$ the eigenvalues of $\tilde{A}$. For the kth mode the time multiplier

$$e^{-\zeta_k \Omega_k t} \sin(\omega_k t) \tag{18}$$

is acting during a free decaying motion. It is characterized by the frequency ω_k (in rad/s) and relative damping ratio ζ_k. These modal parameters are associated with a complex conjugate eigenvalue pair from the real matrix A such that

$$\omega_k = \mathrm{Im}(\log \lambda_k) f \tag{19}$$

$$\zeta_k = -\mathrm{Re}(\log \lambda_k) f / \Omega_k \tag{20}$$

$$\Omega_k = \omega_k / \sqrt{1 - \zeta_k^2} \tag{21}$$

where λ_k is the eigenvalue with positive imaginary part of the two complex conjugate eigenvalues.

4. RESULTS

A preparation of the output data was made before the system identification was performed. The data were resampled (decimated by a factor two) at a lower sampling rate (256 Hz) without intermediate filtering. A few (2 to 5) leading zero-output samples were retained in the data set but the absolute majority of the samples were, of course, samples following the snap-back triggering. A total of 600 samples were used in the identification. All output signals were normalized (pre-conditioned) such that they were of equal 2-norm. A division of the output channels into one estimation set and one validation set was made. In the estimation set outputs from six wing, five nacelle and two fuselage accelerometers were collected. The outputs from two wing, one nacelle and one fuselage accelerometer composed the validation data set.

The acceleration response to the snap-back excitation is triggered by the almost instantaneous release of cable tension. Thereafter the accelerations are governed by the free decay properties of the structure. In the identification procedure we were using a model of the excitation which consisted of a short duration pulse load to trigger the model response. The pulse duration was set to be similar to the duration of the load release, i.e. 6 ms.

Both the ERA and N4SID algorithms have been applied to the data. Stabilization diagrams are shown in figure 4. Consistent results were obtained by the two methods except for a few modes. The most probable cause to that deviation is that these modes were barely controllable by the excitation or observable by the selected distribution of accelerometers.

The identified resonance frequencies and dampings of a model of order 22 (i.e. 11 pairs of complex conjugate modes) are given in Table 1. Table 2 gives the modal assurance criterion (MAC) numbers for a comparison of mode shapes obtained in the normal mode test and after identification using the two methods. In Table 2 only the modes corresponding to resonances up to 40 Hz have been considered since the GVT was restricted to this range. Comparative plots of selected responses involving both low and high frequency modes are shown in figure 2.

The stabilization diagrams show that for a model of order 22 the quality measure Q evaluated on estimation data is 0.711 and 0.710 for models estimated by ERA and N4SID respectively (after re-estimation of B and D). Evaluated on validation data Q increased to 0.793 (N4SID) and 0.792 (ERA) which indicates that the system dynamics are well described by the model.

Prediction error minimization using the described parameterization was then applied using the N4SID estimated model as an initial estimate. After an initial loss of quality (Q=0.696) following the low order parameterization (D becomes constrained), the quality was regained and increased using PEM. After the minimization Q was 0.737 evaluated on the estimation data and to 0.812 using the validation data.

5. CONCLUSIONS

We have found that all three methods give good results in terms of estimated vibrational modes. N4SID and ERA together with PEM also lead to models that in simulation can reproduce the measurements very well. ERA and N4SID give quickly good results. PEM takes more time in these cases where many parameters are being estimated (several

Table 1. Resonance frequencies and dampings of models of order 22 identified by ERA, N4SID and PEM.

N4SID f (Hz)	ERA f (Hz)	PEM f (Hz)	N4SID ζ (%)	ERA ζ (%)	PEM ζ (%)
4.08	4.10	4.11	0.49	0.35	0.50
4.33	4.98	4.74	29.7	3.50	0.78
4.94	4.97	4.94	0.18	0.13	0.20
11.42	11.53	10.67	17.22	1.04	16.90
11.88	11.87	11.87	1.32	1.28	1.16
16.58	16.58	16.58	1.21	1.22	1.16
31.68	30.25	34.39	14.1	1.30	12.99
37.35	37.08	36.98	3.25	4.43	1.8
58.45	51.09	58.26	0.88	34.4	1.15
60.40	58.51	60.41	0.31	0.89	0.42
97.08	60.42	113.0	48.9	0.31	14.42

Table 2. Resonance frequencies and correlation of modes (MAC) given by the ERA and N4SID algorithms and obtained during the normal mode test (GVT).

ERA (Hz)	N4SID (Hz)	GVT (Hz)	ERA/ N4SID MAC	ERA/ GVT MAC	N4SID/ GVT MAC
4.10	4.08	4.22	0.98	0.88	0.86
4.98	4.33	5.63	0.46	0.64	0.87
4.97	4.94	5.76	0.98	0.89	0.91
11.52	11.42	–	0.60	–	–
11.87	11.88	12.05	0.99	0.88	0.88
16.58	16.58	16.89	0.99	0.94	0.95
30.25	31.68	–	0.62	–	–
–	37.35	37.91	0.99	–	0.75
37.09	–	38.0	–	0.72	–

hundreds). On the other hand, such iterations lead to a clear improvement (by 2.5%) of fit on validation data

We may also point to the somewhat unconventional division into validation and estimation sets. In this case with a transient experiment and many (21) outputs we found it better to use the whole time record, but with a selected configuration of output signals, as estimation data and the whole time record with another set of outputs as validation data. This worked very well in our application.

We also found a significant improvement of the fit if we re-estimated B and D after ERA and N4SID. Since these matrices appear linear in the outputs, keeping the rest constant, they can be estimated using an ordinary least-squares solution.

The complex parameterization introduced decreases the numerical complexity substantially when using PEM and also when estimating B and D, since calculating the output of this complex realization is extremely simple with all states independent.

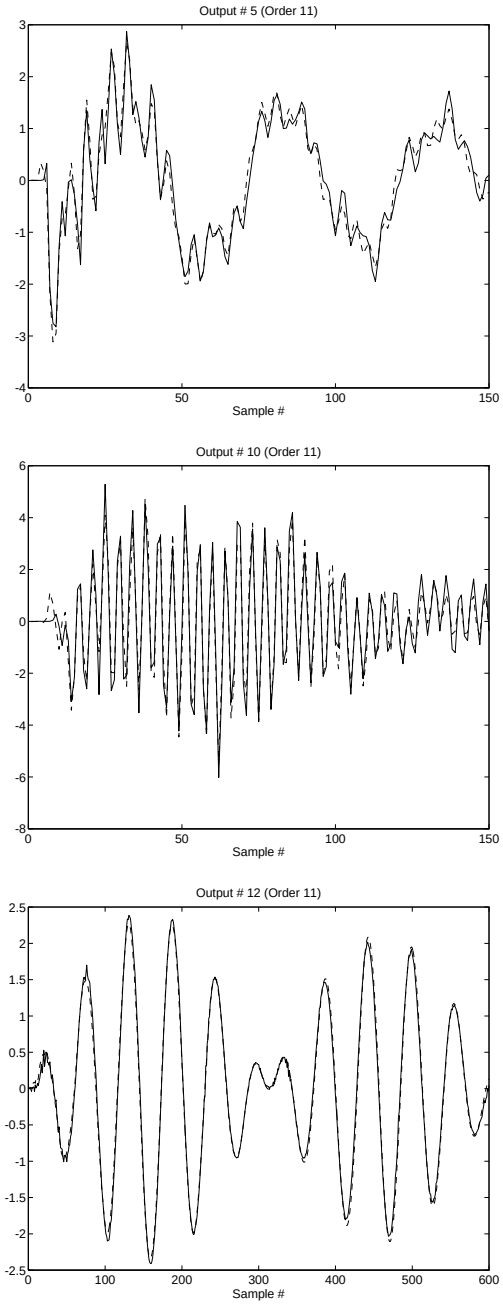

Fig. 2. Selected measured (solid) and simulated (dashed) normalized accelerations. Significantly different frequency contents can be observed. Notice the different time scales. Top graph shows wing tip vertical acceleration. Middle graph shows nacelle lateral acceleration and bottom graph shows vertical acceleration of rearmost fuselage.

6. REFERENCES

Ho, B. L. and Kalman, R. E. (1966). Effective construction of linear state-variable models from input/output functions. *Regelungstechnik*, 14(12):545–592.

Juang, J. N. and Pappa, R. S. (1985). An eigensystem realization algorithm for modal parameter identification and model reduction. *J. of Guidence, Control and Dynamics*, 8(5):620–627.

Ljung, L. (1987). *System Identification: Theory for the User*. Prentice-Hall, Englewood Cliffs, New Jersey.

Van Overschee, P. and De Moor, B. (1994). N4sid: Subspace algorithms for the identification of combined deterministic-stochastic systems. *Automatica*, 30(1):75–93.

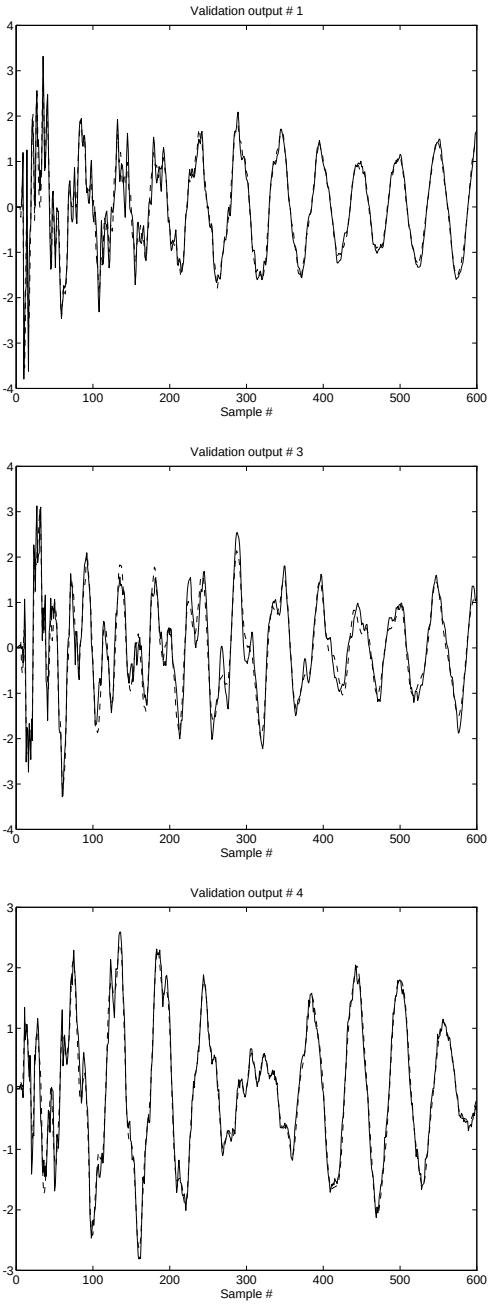

Fig. 3. Selected measured (solid) and simulated (dashed) normalized accelerations used for model validation. Top graph shows vertical acceleration of wing just outboard nacelle. Middle graph shows vertical acceleration of starboard nacelle and bottom graph shows fuselage (just behind wing attachment) vertical acceleration.

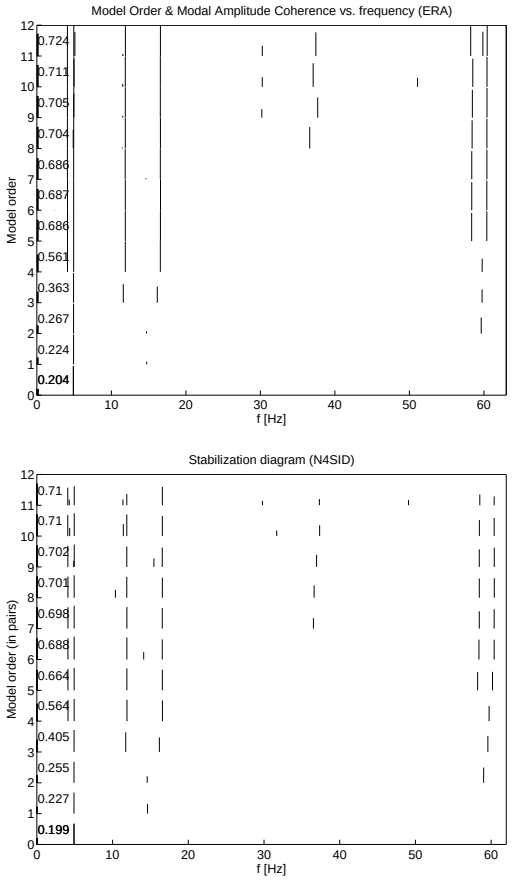

Fig. 4. Stabilization diagrams indicating identified resonance frequencies (as solid lines) vs. model order. Length of lines are equal to Modal Amplitude Coherence γ of identified mode. Normalized estimation error Q at given model order are shown as solid lines on the ordinate axis and also given as numbers. ERA top diagram and N4SID bottom diagram.